PARAMETERS CONTROLLING CARBON FOAMING PROCESSING

Ahmed Elgafy [1], Khalid Lafdi [2]

Abstract *— Incorporating the advantages inherent in both cellular and carbonaceous materials, carbon foam has been considered as a material of great promise, especially in thermal management systems, due to its attractive specific properties. Nevertheless, achieving tailored carbon foams is still a challenging task. Accomplishing this goal would be feasible by recognizing and manipulating the factors that affect the growth of multiple bubbles within bulk molten precursor during the expansion process as it happens inside the foaming reactor. Accordingly, the present study is proposed as an attempt to reach this goal numerically. The volume of fluid, VOF, model based on Euler-Euler Multiphase flow approach has been used as a surface-tracking technique for the interface between the liquid and gas phases. Multiple gas bubbles have been created and distributed within the bulk molten precursor, while the present model has been solved under different pressure and viscosity levels for the sake of parametric study.*

Index Terms — Carbon foams, bubble growth, volume of fluid, multiphase.

INTRODUCTION

Incorporating the advantages inherent in both cellular and carbonaceous materials, carbon foam is a material of great promise due to its attractive specific properties. With a specific modulus rivaling that of a Kevlar honeycomb and a specific conductivity over five times that of copper, the material has naturally been suggested for an eclectic variety of applications [1]. Such applications include heat sinks for electronic chips, heat exchangers, heat pipes and radiators in motor vehicles [2] as well as sandwich structures, aircraft brakes, rocket nozzles and leading edges of aircrafts [3]. Additionally, the development of carbon foam by using raw coal, coal tar pitch and petroleum pitch provides an economical way to produce the next generation lightweight carbon material [4]. However, manufacturing of foam based nanocomposites has been proposed recently for superior foam characteristics, [5,6].

Carbon foam is typically produced by a sudden release of pressure in a supersaturated solution of gas in a molten precursor [7]. With the release of pressure, bubbles form in the melt and begin to grow due to exchanges of mass, momentum, and energy between the melt and this new vapor phase. This growth determines the microstructure, and as such, the thermal, mechanical, and electrical properties of the subsequent foam. Thus, tailoring of the foam is dependent on the ability of controlling the vapor phase bubble growth, a feat possible only with a thorough understanding of the forces at work during the foam formation.

Due to the demanding nature of the problem, there have been several different approaches employed to best model the bubble growth [8-13]. Yet, this growth will not occur at a fixed position in the bulk liquid. During the expansion process, and due to buoyancy forces, the bubble will not expand in a fixed position, but instead it will experience a movement simultaneously with the growth. To validate this hypothesis, Rosebrock et al. [1] introduced a numerical study to comprehend growth and movement of spherical bubble during foam processing. The used numerical model was based on a level set technique for capturing the phase interface. The predicted findings verified that the bubble experiences a movement simultaneously with the growth until the liquid pitch approaches its solid state.

On the other hand, modeling of carbon foam strength characteristics is highly dependent on the idealized structure, which is chosen for the model. Nevertheless, most of these approaches consider foam structure as an open network of triangular struts arranged to form pentagons which fit together to form a dodecahedra or tetrahedral shape [11-13]. This type of structure assumes completely spherical bubbles, an assertion which is not correct [14]. Accordingly, Beechem et al. [15] introduced a numerical study to predict the growth mechanism of a non-spherical bubble assisted for carbon foam fabrication process. In this context, an approach for two dimensional non-spherical mass-diffusion controlled bubble growth in an isothermal Newtonian liquid of infinite extent was considered. A parametric study highlighting the effects of the non-spherical growth of the bubble was performed in order to emphasize how controlled bubble growth can be achieved. At the end of their study, they reported that future work could be initiated concerning the influence of additional bubbles on non-spherical growth in order to further deepen the knowledge concerning the topic of controlled bubble growth.

As seen from revealed literature, growth of an individual bubble within finite or infinite extents of media has been considered to characterize foaming process under certain conditions of particular parameters. Apparently, considering this approach would provide an understanding for bubble growth during foaming process. Yet, it does not offer an integrated perceptive for the entire process, a perspective

1 Ahmed Elgafy, Visiting Assistant Professor, Mechanical Engineering Technology Department, College of Engineering and Applied Science, University of Cincinnati, Admin Building, Room 623, 2220 Victory Parkway Ave, Cincinnati, OH 45206, USA, ahmed.elgafy@uc.edu
2 Khalid Lafdi, Professor, University of Dayton Research Institute, 300 College Park, Dayton, OH 45469, Khalid.lafdi@udri.udayton.edu

that would assist achieving tailored carbon foams. Accomplishing this goal would be feasible by recognizing and manipulating the factors that affect the growth of multiple bubbles within bulk molten precursor during the expansion process as it happens inside the foaming reactor.

The present work is a numerical study to predict and investigate the factors that affect the growth of multiple bubbles within bulk molten precursor during the foaming process. The volume of fluid, VOF, model based on Euler-Euler Multiphase flow approach is used as a surface-tracking technique for the interface between the liquid and gas phases. A single set of momentum equations is shared by the two phases, and the volume fraction of each the phases in each computational cell is tracked throughout the domain.

NUMERICAL FORMULATION

Physical domain

The physical domain is selected to be a foaming reactor, which contains bulk molten precursor. The reactor is supposed to be made of stainless steel that has a cylindrical shape with inner diameter of D_R and height of H_R. The reactor neck, on which a valve is supposed to be hooked, has d_n inner diameter and h_n height. A bulk molten precursor with height of L rests on the bottom of the reactor, while compressed gas occupies the residue of the entire volume of the reactor. To predict and investigate the factors that affect the growth of the bubbles during the expansion process, multiple gas bubbles have been created and distributed within the bulk molten precursor. Due to symmetry, only one half of this domain is considered, Figures 1&2. The system is further defined under the following assumptions: the bubbles have initially a spherical shape and radius of r_b, while their growth is assumed to take place in a Newtonian incompressible fluid. The gas inside the bubbles follows the ideal gas law and its pressure equals that at the interface.

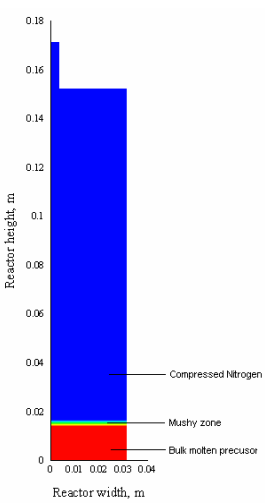

FIGURE. 1
PHYSICAL DOMAIN.

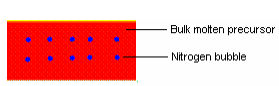

FIGURE. 2
BUBBLES DISTRIBUTION WITHIN MOLTEN PRECURSOR.

The listed values in Table I represent different design parameters and precursor properties for present case of study, while nitrogen represents the gas phase inside both the reactor and the bubbles.

TABLE I
DESIGN PARAMETERS AND PRECURSOR PROPERTIES

Parameter	Symbol	Value	Property	Symbol	Value
Reactor inner diameter	D_R	0.065m	Precursor density	ρ	1260 kg/m, [14]
Reactor height	H_R	0.175m	Precursor specific heat	C_p	2721 J/kg.K, [14]
Reactor neck diameter	d_n	0.01m	Precursor thermal conductivity	k	10 W/m.K, [14]
Reactor neck height	h_n	0.015m	Precursor dynamic viscosity	μ	1 Pa.s, [16]
Molten precursor height	L	0.015m			
Inital bubble radius	r_b	500 μm			

Model description and governing equations

The VOF model can model two or more immiscible fluids by solving a single set of momentum equations and tracking the volume fraction of each of the fluids throughout the domain. The VOF formulation relies on the fact that two or more fluids (or phases) are not interpenetrating. For each additional phase that you add to your model, a variable is introduced: the volume fraction of the phase in the computational cell. In each control volume, the volume fractions of all phases sum to unity. The fields for all variables and properties are shared by the phases and represent volume-averaged values, as long as the volume fraction of each of the phases is known at each location. Thus the variables and properties in any given cell are either purely representative of one of the phases, or representative of a mixture of the phases, depending upon the volume fraction values.

The volume fraction equation

The tracking of the interface(s) between the phases is accomplished by the solution of a continuity equation for the volume fraction of one (or more) of the phases. For the qth phase, this equation has the following form:

$$\frac{\partial \alpha_q}{\partial t} + \vec{v} \cdot \nabla \alpha_q = \frac{S_{\alpha_q}}{\rho_q} \qquad \text{.....(1)}$$

By default, the source term on the right-hand side of equation (1) is zero. The volume fraction equation will not be solved for the primary phase; the primary-phase volume

$$\sum_{q=1}^{n} \alpha_q = 1 \qquad \text{.....(2)}$$

fraction will be computed based on the following constraint:

$$\rho = \alpha_2\rho_2 + (1-\alpha_2)\rho_1 \quad \text{.....(6)}$$

The momentum equation

A single momentum equation is solved throughout the domain, and the resulting velocity field is shared among the phases. The momentum equation, shown below, is dependent on the volume fractions of all phases through the properties α and μ.

$$\frac{\partial}{\partial t}(\rho\vec{v}) + \nabla\cdot(\rho\vec{v}\vec{v}) = -\nabla p + \nabla\cdot\left[\mu\left(\nabla\vec{v} + \nabla\vec{v}^{\mathrm{T}}\right)\right] + \rho\vec{g} + \vec{F} \quad \text{...(3)}$$

The energy equation

The energy equation, also shared among the phases, is shown below.

$$\frac{\partial}{\partial t}(\rho E) + \nabla\cdot(\vec{v}(\rho E + p)) = \nabla\cdot(k_{\mathrm{eff}}\nabla T) + S_h \quad \text{.....(4)}$$

The VOF model treats energy, E, and temperature, T, as mass-averaged variables:

$$E = \frac{\sum_{q=1}^{n}\alpha_q\rho_q E_q}{\sum_{q=1}^{n}\alpha_q\rho_q} \quad \text{.....(5)}$$

where E_q for each phase is based on the specific heat of that phase and the shared temperature. The properties ρ and k_{eff} (effective thermal conductivity) are shared by the phases. The source term, S_h, contains contributions from radiation, as well as any other volumetric heat sources.

Properties

The properties appearing in the transport equations are determined by the presence of the component phases in each control volume. In a two phase system, for example, if the phases are represented by the subscripts 1 and 2, and if the volume fraction of the second of these is being tracked, the density in each cell is given by:

RESULTS

The present model has been solved under different pressure and viscosity levels to investigate and predict the factors that affect the growth of multiple bubbles within bulk molten precursor during the foaming process. The reactor pressure has been varied from 2 MPa to 9 MPa, while molten precursor viscosity has been varied from 1 Pa.s to 2 Pa.s.

Effect of changing of reactor pressure and molten precursor viscosity

Vorticity magnitude

Figures 3, and 4 show the contour lines of vorticity magnitude for different pressure levels for a molten precursor viscosity of 1, and 2 Pa.s respectively. As shown from the figures the vorticity magnitude increases with the increase of pressure. While more turbulence has been noticed with this increase, which would affect the growth of the bubbles directly.

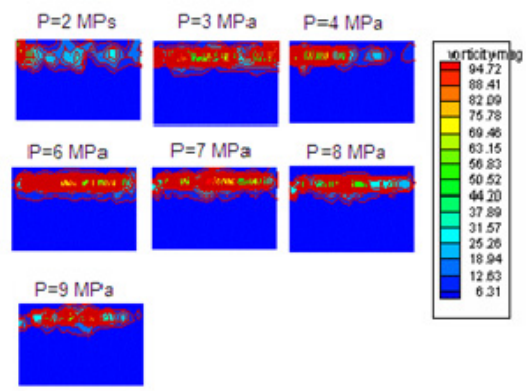

FIGURE. 3

VORTICITY MAGNITUDE, μ = 1 PA.S.

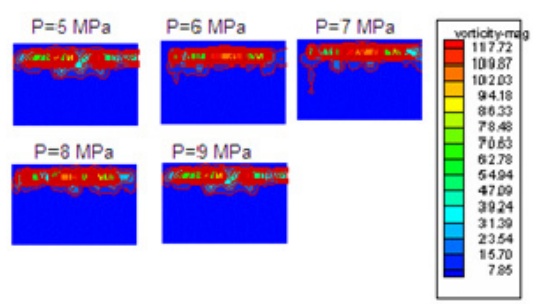

FIGURE. 4

VORTICITY MAGNITUDE, μ = 2 PA.S.

Volume of gas phase

Figure 5, 6, and 7 show the volume of gas phase inside the bubbles for the same previous conditions. As shown from the figures the volume of the gas phase increases with the increase of applied pressure on the reactor. While, the bubbles size decreases with the increase of viscosity.

FIGURE. 5

VOLUME OF GAS PHASE, $\mu = 1$ PA.S.

FIGURE. 6

VOLUME OF GAS PHASE, $\mu = 1.5$ PA.S.

FIGURE. 6

VOLUME OF GAS PHASE, $\mu = 2$ PA.S.

Cells Reynolds number

Figures 7, 8, and 9 show cells Reynolds number for the same previous conditions. As shown from the figures, cells Reynolds number increase with increase of pressure, which would accelerate the expansion process of the bubbles. While, it decreases with increase of viscosity.

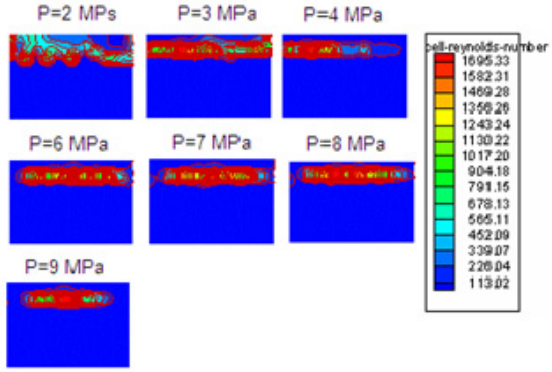

FIGURE. 7

CELLS REYNOLDS NUMBER, $\mu = 1$ PA.S.

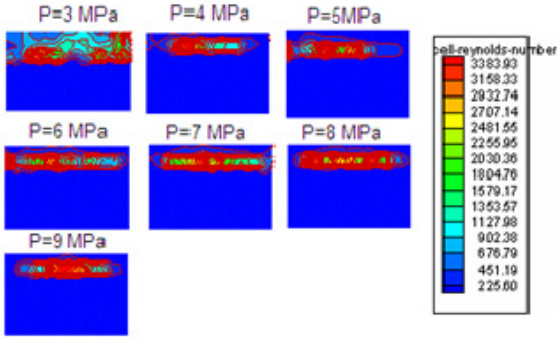

FIGURE. 8

CELLS REYNOLDS NUMBER, $\mu = 1.5$ PA.S.

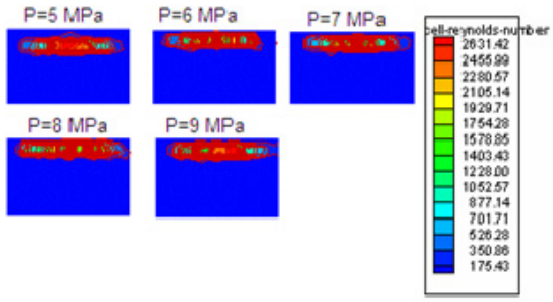

FIGURE. 9

CELLS REYNOLDS NUMBER, $\mu = 2$ PA.S.

Internal Energy for different pressure levels and maximum viscosity

Figure 10 shows the contour lines for the internal energy around and inside the bubbles for different pressure levels and for a viscosity of 2 Pa.s.

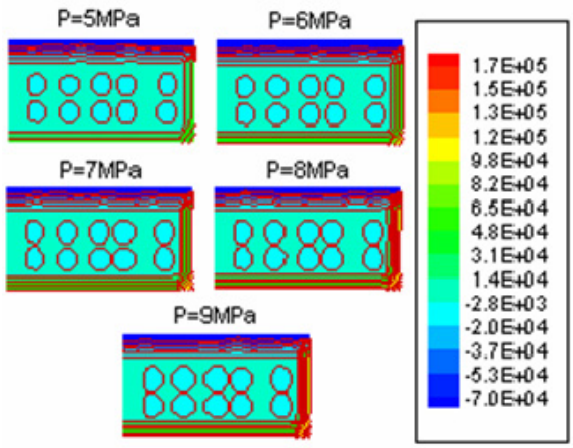

FIGURE. 10

CONTOUR LINES FOR THE INTERNAL ENERGY AROUND AND INSIDE THE BUBBLES FOR DIFFERENT PRESSURE LEVELS, $\mu = 2$ PA.S.

The figure shows that at low pressure levels the bubbles volumes are smaller than that of high pressure levels. Additionally, the bubbles start to coalesce with each other in high pressure levels, which mean that the formation of carbon foam ligaments would be controlled by adapting the pressure level.

CONCLUSIONS

A numerical study based on the volume of fluid, VOF, model has been introduced to investigate and predict the factors that affect the growth of multiple bubbles within bulk molten precursor during the foaming process as it happens inside the foaming reactor. In this context multiple gas bubbles have been created and distributed within the bulk molten precursor, while the present model has been solved under different pressure and viscosity levels for the sake of parametric study. The predicted results show that changing the location of the expansion valve would change the expansion process of the bubbles. The volume of the gas phase increases with the increase in applied pressure on the reactor, while the bubbles size decreases with the increase of viscosity. More than that, the bubbles start to coalesce with each other in high pressure levels, which mean which means that the formation of carbon foam ligaments would be controlled by adapting the pressure level.

Based on the primary results taken from present study, extensive studies would be performed to include more reactor design factors as well as modification of the initial and boundary conditions for the expansion process.

REFERENCES

[1] Rosebrock Gregory, Elgafy A, Beechem T, Lafdi K. Study of the growth and motion of graphitic foam bubbles. Carbon 2005; 43:3075–3087.

[2] Garman RW, Elwell RJ. Thermal performance of a graphite foam material with water flow for cooling power electronics. PCIM conference, Chicago, IL, USA, 2001.

[3] Morgan DR, Biggers SB, Grujicic M. Carbon foam thermal protection systems for space applications. In: Engineering, construction, and operations in challenging environments. Houston, TX, USA: ASCE; 2004.

[4] Chen C, Kennel EB, Stiller AH, Stansberry PG, Zondlo JW. Carbon foam derived from various precursors. Carbon 2006; 44:1535–1543.

[5] Ema Y, Ikeya M, Okamoto M. Foam processing and cellular structure of polylactide-based nanocomposites. Polymer 2006; 47:5350–5359.

[6] Beechem T, Lafdi K. Novel high strength graphitic foams. Carbon 2006; 44:1548–1559.

[7] Shafi MA, Joshi K, Flumerfelt RW. Bubble size distributions in freely expanded polymer foams. Chem Eng Sci 1997;52(4):635–44.

[8] Hall RB, Hager JW. Performance limits for stiffness-critical graphitic foam structures. Part I: Comparisons with high-modulus foams, refractory alloys and graphite epoxy composites. J Compos Mater 1996;30(17):1922–1937.

[9] Joshi K, Lee JG, Shafi MA, Flumerfelt RW. Prediction of cellular structure in free expansion of viscoelastic media. J Appl Polym Sci 1998;67:1353–1368

[10] Venerus D. Diffusion-induced bubble growth in viscous liquids of finite and infinite extent. Polym Eng Sci 2001;41:1390–1398

[11] Hager JW. Idealized strut geometries for open celled foams. Mater Res Soc Proc, San Francisco, CA, 1992. p. 41–46.

[12] Anderson DP, Gunnison KE, Hager JW. Ligament structure of open-cell carbon foams and the construction of models based on that structure. Mater Res Soc Proc, San Francisco, USA, 1992. p. 47–52.

[13] Hager JW, Anderson DP. Idealized ligament formation and geometry in open celled foams. In 21st Biennial Conference on Carbon. Univ. of New York at Buffalo: American Carbon Society; 1993, p. 102–107.

[14] Beechem T. Growth mechanism and properties of novel carbon nanocomposite foams. Master Thesis, University of Dayton, Dayton, Ohio, 2005.

[15] Beechem T, Lafdi K, Elgafy A. Bubble growth mechanism in carbon foams. Carbon 2005; 43:1055–1064.

[16] Khandarea PM, Zondlob JW, Stansberryb PB, Stillerb AH. Rheological investigations of pitch material Part II: viscosity measurement of A240 and ARA-24 pitches using a high-temperature high-pressure rheometer. Carbon 2000; 38: 889–897.